Photoequilibrium in the Primary Steps of the Photoreceptors Phytochrome A and Photoactive Yellow Protein

Thomas Gensch,[†] Klaas J. Hellingwerf,[‡] Silvia E. Braslavsky,*[,†] and Kurt Schaffner[†]

Max-Planck-Institut für Strahlenchemie, Postfach 101365, D-45413 Mülheim an der Ruhr, Germany, and Department of Microbiology, E.C. Slater Institute, University of Amsterdam, NL-1018 WS Amsterdam, The Netherlands

Received: September 9, 1997; In Final Form: December 5, 1997

The photochromic equilibria between the ground state and the first intermediate of the native photoreceptors phytochrome A (phyA) of oat and photoactive yellow protein (PYP) of *Ectothiorhodospira halophila* have been studied by laser-induced optoacoustic spectroscopy, employing photon densities sufficiently high to reach saturation and to establish the photoequilibria between the red-light-absorbing phyA form, P_r, and the first intermediate, I_{700}, and between the PYP ground state, pG, and the first intermediate, pR. The parameters for the photoequilibria $P_r \rightleftarrows I_{700}$ and pG $\rightleftarrows$ pR were determined by the fluence saturation curves of the structural volume change, ΔV_r, analyzed with model functions taking photoselection into account. The quantum yield of the photoreversion, $\Phi_{I700\rightarrow Pr} = 0.22 \pm 0.12$, proved to be ca. 1.4 times larger than the known quantum yield of the forward photoreaction (assuming $\Phi_{Pr\rightarrow I700} = \Phi_{Pr\rightarrow Pfr}$). This suggests that the chromophore-binding protein domain structures of P_r and I_{700} are quite similar. In contrast, the photoreversion quantum yield in PYP for pR → pG is small ($\Phi_{pR\rightarrow pG} = 0.07$) compared with the known value for the thermal forward process to the signaling state pB ($\Phi_{pG\rightarrow pR} \geq \Phi_{pG\rightarrow pB} = 0.35$). This is tentatively attributed to a main conformational change associated with the pG → pR phototransformation. The results of this study emphasize the need of considering photoequilibria in photoreceptors when working with high-fluence laser pulses.

Introduction

Most photosensor chromoproteins have in common a photoisomerizable chromophore as a prosthetic group. The fast photoisomerization (typically in the femto-to-picosecond domain) triggers slower changes of the protein conformation, eventually leading to the signal transduction chain. This feature is common to retinal proteins,[1,2] the photoactive yellow protein (PYP),[3] and the phytochromes.[4]

In each of these photoreceptors at least the primary photochemical product(s), and in certain cases also subsequent intermediates, are formed within a few picoseconds. Irradiation with a nanosecond pulse leads therefore also to the excitation of these intermediates within the pulse time width. As a consequence, these intermediates may be photoisomerized back to the starting material. Indeed, the photochemical back reaction of the K intermediate to bacteriorhodopsin (BR) is even more efficient than the forward photoreaction ($\Phi_{BR\rightarrow K} = 0.64$; $\Phi_{K\rightarrow BR} = 0.94$).[5]

Recently, we have determined the structural volume changes associated with the primary phototransformation steps of the plant phytochrome A (phyA)[6,7] and of eubacterial PYP[7,8] by laser-induced optoacoustic spectroscopy (LIOAS) measurements at several temperatures.

The pressure pulse detected by LIOAS is the sum of two contributions to the total volume change induced in the solution, viz., thermal deactivation of the excited molecules, ΔV_{th}, and structural changes, ΔV_r.[9,10] The value of ΔV_{th} linearly depends on the ratio of thermoelastic parameters of the medium ($\beta/(c_p\rho)$, with β = cubic expansion coefficient, c_p = heat capacity, and ρ = mass density), while ΔV_r is independent of these parameters. Since in water β equals zero at $T_{\beta=0} = 3.9$ °C, which amounts to $\Delta V_{th} = 0$, LIOAS measurements of aqueous solutions at this temperature permit a direct study of ΔV_r. This offers an interesting access to the analysis of photochromic reactions. The ΔV_r value should reach saturation with increasing laser fluence and as a function of the photoproduct concentration. In other words, ΔV_r saturation occurs as a function of the quantum yields of the forward and backward reactions. Since the ΔV_r values are identical, but of opposite sign, in the two directions of a photochromic reaction, the values of the saturation level ΔV^{satd} and curvature b [eq 2 vide infra] will be influenced by the photoequilibrium kinetics. The monitoring of ΔV_r fluence saturation at $T_{\beta=0}$ has already been exploited in studies of photosynthetic reaction centers.[11−12]

The primary step of the phototransformation of the red-light-absorbing form of phyA, P_r, to the first intermediate, I_{700}, is accompanied by an expansion of $\Delta V_e = 0.9$ mL per mol of absorbed photons,[6,7] while the corresponding photoreaction of PYP, pG → pR, shows a contraction of $\Delta V_e = -5.0$ mL per mol of absorbed photons.[7,8] These measurements were performed at photon densities that were within the linear fluence dependence of the LIOAS signal and converted less than 10% of the molecules in the irradiated volume.

All members of the phytochrome family[13] have molecular weights of around 120 kDa/monomer.[14] In solution they exist as dimers. They possess an open-chain tetrapyrrole chromophore, phytochromobilin, covalently attached to a cysteine of the protein backbone through a thioether bond. The photochromism, interconverting the two stable forms P_r ($\lambda_{max} \approx 665$ nm) and P_{fr} ($\lambda_{max} \approx 730$ nm), is an inherent property of the monomeric chromoprotein.[4,14] It is initiated by *Z*,*E* isomer-

[†] Max-Planck-Institut für Strahlenchemie.
[‡] University of Amsterdam.

S1089-5639(97)02944-7 CCC: $15.00
Published on Web 01/27/1998

ization of one of the phytochromobilin double bonds. Excitation of P_r, which is the more extensively investigated form to present, leads to the formation of several intermediates with lifetimes in the micro-to-millisecond domain.[4,15] Although the number of intermediates, their spectral properties, and the reaction scheme are still under debate,[16−18] it is generally accepted that a primary photoproduct with a red-shifted absorption maximum and an increased absorption coefficient, called lumi-R or I_{700}, is formed in less than 200 ps.[19−22] It decays thermally en route to P_{fr} with biexponential kinetics in the microsecond time range (8 and 90 μs at 10 °C) to I_{bl}.[17] The latter is a transient with lower absorption coefficients throughout the entire absorption spectrum.

The primary photoreaction, $P_r \rightarrow I_{700}$, is photoreversible.[17,23] Since the absorption spectra of P_r and I_{700} strongly overlap, a photoequilibrium $P_r \rightleftarrows I_{700}$ is established at sufficiently high excitation fluences and at excitation durations that are long in comparison with the growth kinetics of I_{700} (ca. 50 ps).[19,20] Should this photoequilibrium be neglected, photophysical investigations would risk erroneous interpretation.

PYP is the second photoreceptor that we have now subjected to a fluence-saturation study of ΔV_r at $T_{\beta=0}$. It is a water-soluble 14-kDa chromoprotein that acts as a sensor for the negative phototactic response of *Ectothiorhodospira halophila* toward blue light (450 nm).[24] Its chromophore is the deprotonated *p*-coumarylthiol ester linked to a cysteine.[25−27] After excitation of pG, the stable state of PYP at room temperature, the intermediate pR is formed within 3−12 ps,[28,29] presumably by an $E \rightarrow Z$ isomerization of the chromophore double bond.[3] The subsequent thermal pR → pB decay is biexponential and is completed within about 2 ms. The *Z* chromophore of pB is protonated[3,27] and exhibits a blue-shifted absorption spectrum. Eventually, a thermal $Z \rightarrow E$ isomerization and deprotonation reverts pB back to pG in several seconds.[30] The pB state is believed to be the signaling state.[31]

Although pR and pG have strongly overlapping spectra,[30] pB has virtually no absorption at the maximum of pG (446 nm). This permits the use of pG bleaching after 2 ms of excitation in flash photolysis as a measure of pB formation. Considerably different quantum yields of pB formation, however, have been reported by Meyer et al. and ourselves, i.e., $\Phi_{pG\rightarrow pB} = 0.64$[32] and 0.35,[7,8] with a lower limit of $\Phi_{pG\rightarrow pR} > 0.16$ estimated by LIOAS.[7] A photochemical back reaction, pR → pG, has to be considered also in this system, especially since at low temperatures an intermediate with a red-shifted absorption (490 nm at 77 K) has been detected, which could be photoconverted back to pG.[33]

We now report on a study of $P_r \rightleftarrows I_{700}$ in phyA and pG $\rightleftarrows$ pR in PYP, with photon densities sufficiently high to ascertain fluence saturation and photoequilibrium in each case.

Experimental Section

Native phyA (124 kDa) was isolated from etiolated oat and purified as described by Brock et al.[34] It was dissolved in 10 mM potassium phosphate buffer (pH 7.8), 2 mM ethylenediaminetetraacetic acid, 2 mM dithiothreithol, and 2 mM phenylmethylsulfonyl fluoride. Bromocresol green (Fluka) was used as a calorimetric reference.[35] For the determination of scattering artifacts, a protein suspension of cracked yeast cells (*Pichia pastoris*) was used as a nonabsorbing scattering medium.

The isolation of PYP has been described by Hoff et al.[30] PYP was dissolved in 10 mM Tris buffer (pH 7.8) and 1 mM NaCl. $K_2Cr_2O_7$ was used as the calorimetric reference in the same buffer.

The following sample solutions were measured: phyA at $\lambda_{exc} = 650$ nm, $c = 1.68$ μM, $A(P_r) = 0.16$, and at $\lambda_{exc} = 700$ nm, $c = 4.89$ μM, $A(P_r) = 0.11$; PYP at $\lambda_{exc} = 446$ nm, $c = 2.86$ μM, $A(pG) = 0.13$, at $\lambda_{exc} = 460$ nm, $c = 7.56$ μM, $A(pG) = 0.26$, and at $\lambda_{exc} = 480$ nm, $c = 24.53$ μM, $A(pG) = 0.14$.

The LIOAS signal was detected by a Pb−Zr−Ti ceramic transducer (Minhorst, 4 mm diameter), amplified (100 times, Comlinear E103), digitized by a storage oscilloscope (Tektronix TDS 684, 2 ns/channel), and averaged 25−100 times depending on the signal-to-noise ratio.[10] The data were further treated with a VAX station 3100, a mainframe VAX, and IBM-compatible personal computers.

For the experiments with phyA, two dye lasers were pumped by the 8-ns frequency-doubled pulses of a Q-switched Nd:YAG laser at a 2-Hz repetition rate.[6] The output was used for excitation of P_r and I_{700} (at $\lambda_{exc} = 650$ or 700 nm) and for back conversion of P_{fr} to P_r (at $\lambda_{irr} = 740$ nm). Two shutters were synchronized by computer in order to allow one excitation pulse to impinge on the sample cell for every 90 pulses at 740 nm. The fluence of the excitation light was varied by a neutral-density filter and measured with a pyroelectric energy meter.[6−8] The energy of the 740-nm pulse was about 1 mJ. Its spot coincided with the entire excitation area covered by the 700- and 650-nm pulses.

The spatial profile of the excitation pulse, measured by a Si photodiode and a narrow pinhole (0.05 mm) as a mask, showed a Gaussian distribution in the *x* (perpendicular to the detector surface) and *y* directions (parallel to the detector surface) with fwhms of 2.1 and 1.34 mm, respectively. The excitation beam passed through a slit of 0.8 mm × 4 mm (*x* and *y* directions, respectively).

PYP was excited by the beam of an excimer-laser-pumped dye laser ($\lambda_{exc} = 446$, 460, or 480 nm, 10-ns pulse width, 0.2-Hz repetition rate) with a nearly circular Gaussian profile (1 mm fwhm).[7,8] The excitation beams of 446 and 460 nm passed through a 0.9-mm diameter pinhole, which rendered the distribution of the exciting photons more uniform. The low absorption coefficients of pG and pR at $\lambda_{exc} = 480$ nm necessitated a different setup. To reach saturation, the photon densities had to be increased in comparison to the other experiments. Therefore, the beam was focused with a lens ($f = 500$ mm), and a pinhole of 0.15 mm was placed in the focal point. In this configuration the excitation energy was estimated by measuring the transmitted light after the cuvette and by correcting for the absorption within the cell.

In the calculation of the excited volume V_{exc} the 1-cm path and the dimensions of either slit or pinhole were taken into account. In the experiment with PYP at $\lambda_{exc} = 480$ nm a cylinder of 0.26 mm diameter was taken as V_{exc}.

Results

The temperature $T_{\beta=0}$, required for an appropriate investigation of the saturation behavior of the sample signal, was determined by monitoring the disappearance of the reference LIOAS signal in the given buffer as a function of temperature.[6−8] The LIOAS signal of phyA at this temperature was positive and reflected exclusively the structural volume change of the $P_r \rightarrow I_{700}$ transformation (see Figure 5 in Gensch et al.[6]). The LIOAS-signal of PYP at $T_{\beta=0}$ was negative (see Figure 1 in the work of van Brederode et al.[8]).

In our previous study of phyA[6] we have shown that there is no signal shift or deformation that would result from a contribution of the I_{700} decay in the range 3−20 °C. The same holds for the pR intermediate of PYP.[8] Consequently, no

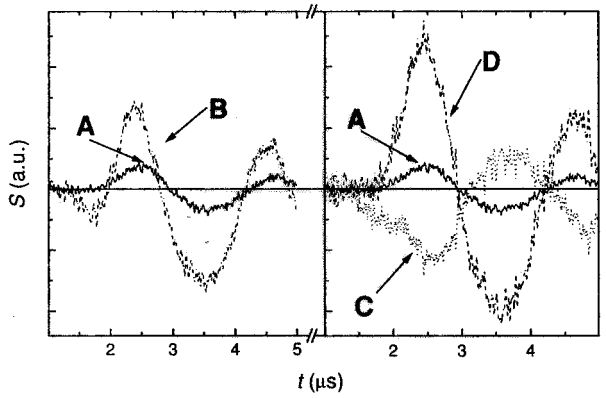

Figure 1. (Left) LIOAS signals of phyA ($T = 2.8$ °C, $\lambda_{exc} = 650$ nm, $A = 0.159$) at $T_{\beta=0}$ at low (curve A, $E_{exc} = 19$ μJ) and high excitation energies (curve B, $E_{exc} = 150$ μJ). (Right) Distortion signal due to light scattering by reference (yeast protein; curve C), normalized to the beginning of curve B, and corrected LIOAS wave D = B − C.

deconvolution was necessary and the amplitude of the first wave of the LIOAS signal could be used. The signal amplitudes of the sample, S^{sample}, at $T_{\beta=0}$ were transformed into ΔV values by using eq 1.[6,7] The $T_{\beta=0}$ values of the two buffers have been estimated already in our previous studies: $T_{\beta=0} = 2.8$[6] and 2.6 °C[8] for the potassium phosphate (phyA) and Tris buffer (PYP), respectively. $T_{\beta\neq0}$ values of 12.5 and 20 °C were chosen for the phyA and PYP experiments, respectively. The absorbances (A) of sample and reference solutions were matched. S_n^{ref} is the fluence-normalized value of the LIOAS amplitude and denotes the slope of the linear plot of reference signal vs excitation energy E_{exc}:

$$\Delta V_r = \frac{S^{sample}_{T_{\beta=0}}}{S^{ref}_{n,T_{\beta\neq0}}} \left(\frac{c_p \rho}{\beta}\right)_{T_{\beta\neq0}} \quad (1)$$

This method is based on the condition that the difference in the isothermal compressibility, κ_T, of the solutions at $T_{\beta=0}$ and $T_{\beta\neq0}$ is negligible. In the case of phyA this assumption is safe. For PYP a correction was necessary in view of the higher $T_{\beta\neq0}$ value. Since the optoacoustic signal is inversely proportional to the compressibility,[10] the ΔV_r values (eq 1) were multiplied for this purpose by the ratio κ_T (3 °C)/κ_T (20 °C) = 1.09 obtained from the respective κ_T values of 4.99×10^{-10} and 4.59×10^{-10} Pa for neat water.[36]

Another assumption, which is conditional to the use of temperature as a variable to separate the structural and thermally produced volume changes, is that ΔV_r, i.e., the structural volume change, is constant in the relatively narrow temperature range monitored. This assumption is justified by the linear dependence of the reference-normalized LIOAS signal intensity at low fluences on $c_p\rho/\beta$ for phyA[6,7] and for PYP.[7,8]

At high fluences, the early part of the LIOAS signal of phytochrome is distorted (Figure 1), unlike the LIOAS waveforms of PYP and the reference samples. Since the distortion started prior to the appearance of the prompt LIOAS signal (data not shown) and intensified with increasing E_{exc}, it is attributed to scattered laser light. This artifact was corrected by subtracting the energy-normalized LIOAS signal of a nonabsorbing yeast protein extract from the phytochrome signal at the higher E_{exc} values (>50 and >25 μJ at 650 and 700 nm, respectively). Figure 1 shows LIOAS waveforms from phytochrome solutions at low and high E_{exc}, as well as the distorted and corrected signals at high E_{exc} (for similar correction procedures see refs 37).

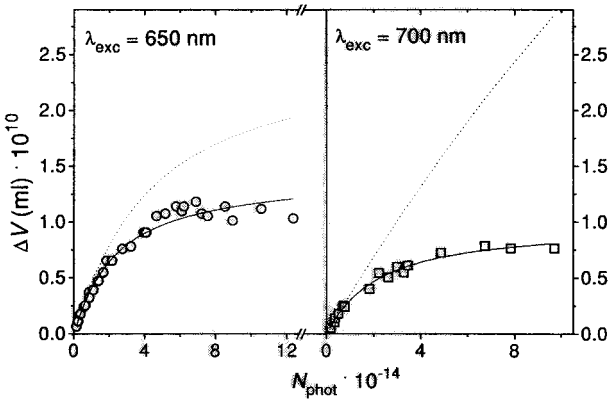

Figure 2. Experimental ΔV_r values of phyA at $T_{\beta=0}$ as a function of incident photons N_{phot}. Left (○): $\lambda_{exc} = 650$ nm, $A_{650} = 0.16$, $N_{phyA} = 3.225 \times 10^{13}$. Right (□): $\lambda_{exc} = 700$ nm, $A_{700} = 0.11$, $N_{phyA} = 9.205 \times 10^{13}$; (−) best fit based on eq 11 (for fit data see Table 1); (···) simulated curve based in Scheme 1 and $\Phi_{Pr\rightarrow I700} = 0.15$ (see Discussion).

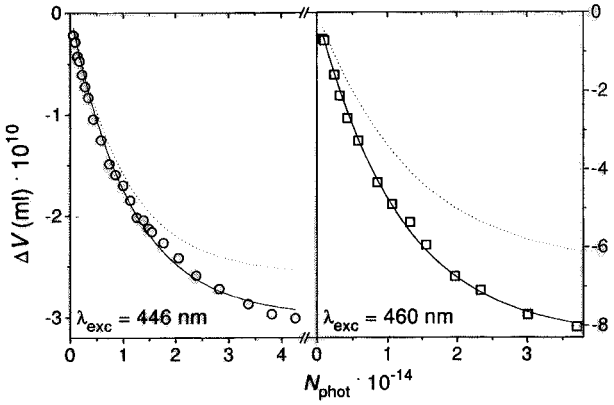

Figure 3. Experimental ΔV_r values of PYP $T_{\beta=0}$ as a function of incident photons N_{phot}. Left (○): $\lambda_{exc} = 446$ nm, $A_{446} = 0.13$, $N_{PYP} = 1.10 \times 10^{13}$. Right (□): $\lambda_{exc} = 460$ nm, $A_{460} = 0.26$, $N_{PYP} = 2.80 \times 10^{13}$); (−) best fit based on eq 2 (for fit data see Table 3); (···) simulated curve based in Scheme 1 and $\Phi_{pG\rightarrow pR} = 0.35$ (see Discussion).

In Figures 2 and 3, the experimental values of ΔV_r at $T_{\beta=0}$, calculated by use of eq 1, are plotted as a function of the number of incident photons per pulse, N_{phot}, at $\lambda_{exc} = 650$ and 700 nm for phyA and $\lambda_{exc} = 446$ and 460 nm for PYP, including fitting and simulated model functions (see Discussion). Since the ratios of the absorption cross sections of P_r to I_{700} and of pG to pR depend on the excitation wavelength, the photochromic equilibrium concentrations of $P_r \rightleftarrows I_{700}$ and pG ⇄ pR also vary with these wavelengths. While in the experiments depicted in Figures 2 and 3 the saturation values were almost achieved, only 65% of the PYP molecules were phototransformed with 480-nm excitation (data not shown) despite the focusing configuration. The results of this latter experiment are therefore less reliable.

Discussion

Choice of Saturation Model. The simplest analysis of saturation experiments is the fitting of a function such as eq 2 to the experimental points of a signal vs N_{phot} plot. Two schemes were evaluated for the application to the experiments in this work: a four-state model (with a starting compound A, a first intermediate B, and both excited species) with and without photochemical reversion. Owing to the short lifetimes of the excited states, $[A]_{t=0}$ at any time t equals $[A]_t + [B]_t$. The

physical meaning of ΔV^{satd} and b depend on which of these two models applies to the system under study. In the absence of a photochromic system (Scheme 1), the parameters of the fluence-dependent data are given by eq 5, while in the presence of a photoequilibrium (Scheme 2) the parameters have the form given by eq 8.

$$\Delta V(N_{phot}) = \Delta V^{satd}\,[1 - \exp(-bN_{phot})] \tag{2}$$

Scheme 1 $\quad A \rightarrow B$

$$\frac{d[A]}{dt} = -E_p \Phi_{A\rightarrow B} \sigma_A [A] \tag{3}$$

$$\frac{d[B]}{dt} = E_p \Phi_{A\rightarrow B} \sigma_A [A] \tag{4}$$

Consequently, in eq 2

$$b = \Phi_{A\rightarrow B}\sigma_A$$

$$\Delta V^{satd} = \frac{\Delta V_e}{\Phi_{A\rightarrow B} N_A} N_{sample} \tag{5}$$

Scheme 2 $\quad A \rightleftarrows B$

$$\frac{d[A]}{dt} = -E_p \Phi_{A\rightarrow B} \sigma_A [A] + E_p \Phi_{B\rightarrow A} \sigma_B [B] \tag{6}$$

$$\frac{d[B]}{dt} = E_p \Phi_{A\rightarrow B} \sigma_A [A] - E_p \Phi_{B\rightarrow A} \sigma_B [B] \tag{7}$$

$$\Delta V^{satd} = \frac{\Delta V_e}{N_A} N_{sample} \frac{\sigma_A}{\Phi_{A\rightarrow B}\sigma_A + \Phi_{B\rightarrow A}\sigma_B} \tag{8}$$

Now, b of eq 2 is given by

$$b = \Phi_{A\rightarrow B}\sigma_A + \Phi_{B\rightarrow A}\sigma_B$$

In these equations, ΔV_e is the structural volume change per mole of absorbed photons ($=\Phi_{A\rightarrow B}\Delta V_R$), N_A is the Avogadro constant, N_{sample} is the number of sample molecules in the excited volume, $\Phi_{A\rightarrow B}$ is the quantum yield of the formation of intermediates ($\Phi_{Pr\rightarrow I700}$ for phyA and $\Phi_{pG\rightarrow pR}$ for PYP), $\Phi_{B\rightarrow A}$ is the quantum yield of the respective back reaction, and $\sigma_A(\lambda)$ and $\sigma_B(\lambda)$ are the absorption cross sections of starting compound A and intermediate B. E_p is the photon irradiance in $cm^{-2}\ s^{-1}$.

Equation 2 describes the saturation behavior (which is defined by the leveling-off of the fluence dependence of the LIOAS signal amplitude) as long as the excitation is virtually isotropic. This condition, in turn, is fulfillled if the excitation energy is uniformly distributed in the excited volume and if either (i) the polarization of the exciting light is isotropic (which is not the case in the present experimental setup) or (ii) the excitation is not isotropic but the absorbing molecules rotate within the duration of the excitation pulse. When the excited molecules do not rotate within the duration of the excitation pulse, they remain virtually immobile during this period and photoselection can occur. However, when they do rotate during this period, photoselection is not observed [condition ii].

A simple description of the rotation of molecules in solution is given by the Einstein−Smoluchovski equation (eq 9),[38] which relates the rotational diffusion time τ_R to the temperature T, the solvent viscosity η, and the solute volume V_s. This equation is valid for

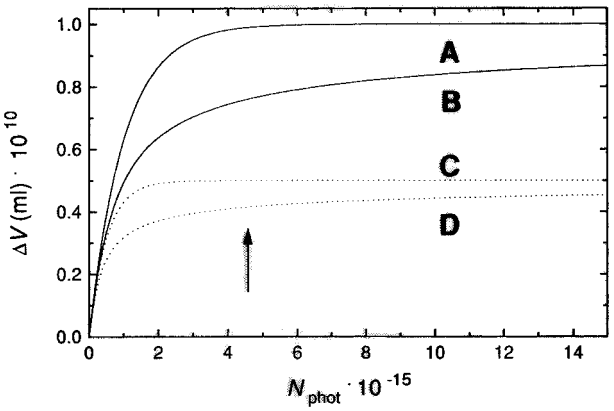

Figure 4. Simulations of ΔV_r with $\Delta V^{satd} = 1.0 \times 10^{-10}$ mL and $b = 1.0 \times 10^{-15}\ cm^{-2}$ as a function of the incident photons N_{phot} without (A, B: $\Phi_{B\rightarrow A} = 0$) and with photochemical back reaction (C, D: $\Phi_{B\rightarrow A} = \Phi_{A\rightarrow B}$, $\sigma_A = \sigma_B$) based on eqs 2 (A, C) and 11 (B, D). The arrow indicates the highest N_{phot} used in the experiments.

$$\tau_R = \frac{\eta V_s}{kT} \tag{9}$$

spherical molecules. The maximal correction for a different geometrical shape is less than 50%.[39] In general, τ_R increases for a less spherical molecule.

In the case of linearly polarized excitation, the saturation behavior becomes a function of the pole distance angle ϑ between **E** and the transition dipole moment $\boldsymbol{\mu}$. For molecules rotating much more slowly than the excitation pulse duration, the saturation function is given by the following integral for $0 < \vartheta < \pi$ (eq 10):

$$\Delta V(N_{photo}) = \int \Delta V^{satd}[1 - \exp(-bN_{photo}\cos\vartheta)]\,d\vartheta \tag{10}$$

Kawato and Kinosita,[40] Nagle et al.,[41] and Kliger et al.[42] have already investigated the different absorption probabilities and saturation behavior for large, slowly rotating units such as purple membrane particles. Integration over ϑ leads to a function describing the saturation behavior of molecules with $\tau_R \gg \tau_{pulse}$ (eq 11).

$$\Delta V(N_{phot}) = \Delta V^{satd}\left[1 - 0.5\sqrt{\frac{\pi}{3bN_{phot}}}\,\mathrm{erf}(\sqrt{3bN_{phot}})\right] \tag{11}$$

Figure 4 shows the different saturation behavior of two samples with identical ΔV^{satd} and b values, for fast (eq 2, curves A and C) and slow rotation (eq 11, curves B and D) compared with τ_{pulse}, and for cases without (Scheme 1, curves A and B) and with photochemical back reaction (Scheme 2, curves C and D). Equation 11 (slow rotation) predicts that B and D deviate earlier from initial linearity and reach the saturation level later than A and C under the regime of eq 2, which is applicable to fast rotation (i.e., no photoselection). It is evident from the plots in Figure 4 that neglect of the photoselection phenomenon in the case of virtually immobile samples would lead to incorrect photophysical parameters.

From eq 9 and the phytochrome dimer dimensions, obtained by electron microscopy and small-angle X-ray scattering, values of $\tau_R = 260$ ns (by using V_s from Jones and Erickson[43]) and 130 ns (by using V_s from Nakasako et al.[44]) can be calculated,[45] neglecting the deviations of the dimer from a perfect sphere.

This calculation ascertains that phyA remains immobile during excitation with an 8-ns excitation pulse, and photoselection ought to be considered because conditions i and ii are not fulfillled. Since the orientations of the absorption dipole moments of P_r and I_{700} are not markedly different (see Savikhin et al.[19]), eq 11 can be used for the simulation of the fluence saturation experiment with phyA.

In the case of PYP, condition ii is fulfillled, since a τ_R value of ca. 6 ns (ie., $\tau_R < \tau_{pulse}$) is calculated from X-ray diffraction crystal-structure data.[26] Photoselection plays no major role because most molecules rotate within the 10-ns excitation pulse. Thus, the fluence saturation experiments with PYP should be analyzed by eq 2.

The a priori condition of uniform excitation distribution will never be fulfillled ideally, since the sample absorbs part of the excitation light, and therefore, the excitation probability decreases exponentially with progression along the light path (Lambert−Beer law). However, this effect should be negligible for the dilute samples studied, since the optoacoustic transducer (with a circular surface of 4 mm diameter) records the integrated signal from the entire illuminated area.

Uneven distribution of the excitation energy in the plane perpendicular to the light beam, which had a Gaussian spatial profile (see Experimental Section), is to be considered a second source of nonuniformity in our experiments. The nonuniform distribution of excited species generated leads to different degrees of saturation within V_{exc}. Equations 12 and 13 describe the saturation behavior of ΔV as a function of the spatial distribution of photons $S(\mathbf{r})$:[12]

$$\int_A \Delta V(N_{phot}, \mathbf{r})\, dA = \int_A \Delta V^{satd}[1 - \exp(-x)]\, dA \qquad (12)$$

$$\int_A \Delta V(N_{phot}, \mathbf{r})\, dA = \int_A \Delta V^{satd}\left[1 - 0.5\sqrt{\frac{\pi}{3x}}\,\mathrm{erf}(\sqrt{3x})\right] dA \qquad (13)$$

$$x = bN_{phot}\frac{S(\mathbf{r})}{\int_A S(\mathbf{r})\, dA}$$

A in this case indicates the irradiated area. In the case of a Gaussian distribution, the saturation starts at lower E_{exc} values in the center of the beam than at the edges. This leads to a faster deviation from linearity at low N_{phot} and to a slower final saturation.

To evaluate the influence of the photon distribution on the results, the fluence dependence of the ΔV_r values was simulated by eq 13 (see Figure 5) with a uniform (○) and with two Gaussian distributions (□) perpendicular (fwhm = 2.1 mm) and parallel (fwhm = 1.34 mm) to the detector surface. The two orthogonal distributions (□) reflect the experimental situation in the phyA investigations. The integration was performed for several values of bN_{phot}[46] and within a fluence range twice the maximum fluence experimentally available (see arrow in Figure 5). Comparison of the two simulations in Figure 5 shows that the deviations from a uniform spatial photon distribution must not be neglected in the phyA experiments. Owing to the relatively narrow slit (0.8-mm width), the differences between the uniform and the Gaussian distribution were very small in the direction perpendicular to the detector surface. However, in the direction parallel to the detector, the differences were more marked because of the relatively large (4 mm) slit height in relation to the fwhm of 1.34 mm.

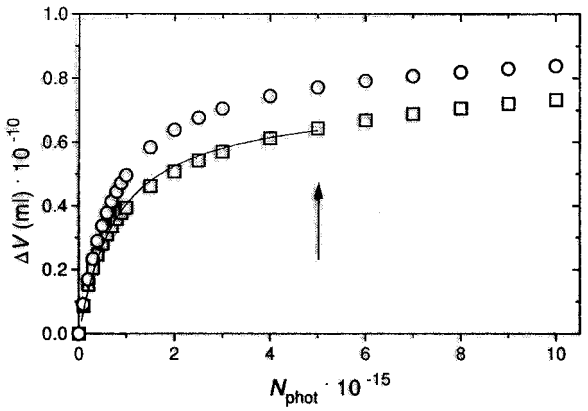

Figure 5. Simulation of ΔV_r by using eq 13, with $\Delta V^{satd} = 1.0 \times 10^{-10}$ mL and $b = 1.0 \times 10^{-15}$ cm^{-2} as a function of the incident photons N_{phot} with uniform (○) and Gaussian-like (□) photon distributions; (−) function fitted to □ by eq 11 (hence, assuming a uniform distribution). The arrow indicates the highest N_{phot} used in the phyA experiments.

As described above, the saturation behavior of the two Gaussian-like photon distributions in the phyA experiment (Figure 5) appears different from that based on eq 11. Since there is no analytical solution for the integral in eq 13, the experimental dependence of ΔV_r on N_{phot} was analyzed on the basis of eq 11, which assumes a uniform photon distribution. This led to incorrect ΔV^{satd} and b values. To correct for the inappropriate fitting function, the simulated curve □ was fitted with eq 11 in the experimentally accessible fluence range. In this way, the values of ΔV^{satd} and b obtained with eq 11 (Figure 2) were estimated to be 15% and 5% lower, respectively, than those that would have been obtained with a uniform distribution. The results obtained from the analysis of the data in Figure 2 were corrected accordingly.

The results with PYP required no correction for an inhomogeneous distribution. In both the nonfocusing and the focusing configurations the pinholes (diameters of 0.9 and 0.15 mm, respectively) were placed in the center of the beam, which rendered the illumination nearly homogeneous.

Once the appropriate function for the analysis of the saturation curve was established [i.e., eq 11 for phyA and eq 2 for PYP], the values of ΔV^{satd} and b could be calculated. In the case that Scheme 1 should prove inapplicable and that data analyzed by eq 5 and the corresponding b value should lead to unreasonable values for the forward quantum yield, $\Phi_{A\rightarrow B}$, the alternative Scheme 2, eq 8, and the corresponding b value were to be applied in order to estimate the backward quantum yield $\Phi_{B\rightarrow A}$ by using an independently determined value of $\Phi_{A\rightarrow B}$.

The difficulties introduced by a nonuniform spatial distribution in the excitation area illustrate the advantage of choosing an area distinctively smaller than the excitation beam cross section for studies under saturating conditions. Therefore, the use of a pinhole instead of a slit is recommended.

Phytochrome. Subnanosecond transient absorption studies carried out previously with phyA indicate that an intermediate with spectral characteristics comparable to those of I_{700} is formed from P_r within 200 ps.[19,20] Moreover, nanosecond studies[16−18] demonstrate the existence of two I_{700} intermediates with similar spectra, both of which decay within time ranges of microseconds. It is not yet clear whether these I_{700} species are formed in a parallel (i.e., simultaneously, $P_r \rightarrow I^1_{700} + I^2_{700}$) or in a sequential manner ($P_r \rightarrow I^1_{700} \rightarrow I^2_{700}$), with either primary step on a picosecond time scale. Both models are compatible with the literature data[15−18] and with the data of the present study.

TABLE 1: ΔV^{satd} and b Values for phyA, Derived from Figure 2 and Eq 11, Together with Literature Values of the P_r and I_{700} Absorption Cross Sections (σ_{Pr} and σ_{I700}, Respectively) and the Number of phyA Molecules N_{phyA} in the Excited Volume

λ_{exc} (nm)	σ_{Pr} (cm^{-2})[a] $\times 10^{16}$	σ_{I700} (cm^{-2})[b] $\times 10^{16}$	b (cm^{-2}) $\times 10^{16}$	ΔV^{satd} (mL) $\times 10^{10}$	N_{phyA} $\times 10^{-13}$
650	3.63	2.65	1.05	1.62	3.225
700	0.86	4.10	1.15	1.11	9.205

[a] Values taken from Kelly and Lagarias.[47] [b] Values taken from Zhang et al.[16]

TABLE 2: Quantum Yields for the Back Reaction $\Phi_{I700\rightarrow Pr}$ and the Forward Reaction $\Phi_{Pr\rightarrow I700}$ of phyA, Calculated from the Values of ΔV^{satd} and b Based on Schemes 1 and 2

Scheme 1 (without Photoequilibrium)

λ_{exc} (nm)	$\Phi_{Pr\rightarrow I700}$[a]	$\Phi_{Pr\rightarrow I700}$[b]
650	0.29	0.30
700	1.34	1.34

Scheme 2 (with Photoequilibrium)

λ_{exc} (nm)	$\Phi_{I700\rightarrow Pr}$[a]	$\Phi_{I700\rightarrow Pr}$[b]
650	0.19	0.20
700	0.24	0.23

[a] Calculated from b. [b] Calculated from ΔV^{satd}.

The experimental points ΔV^{satd} vs N_{phot} fitted by eq 11 are plotted in Figure 2. The ΔV^{satd} and b values, corrected for a spatial Gaussian distribution of the photons in the excitation beam as described above, are given in Table 1 for the two excitation wavelengths. Additionally, a model function is depicted in Figure 2 (···), which has been simulated by using eq 11 and values of ΔV^{satd} and b based on the assumption that Scheme 1 is valid (no back photoreaction). For the calculations, a value of $\Delta V_e = 0.9$ mL/mol from our previous LIOAS study of phyA at low fluences,[6] the absorption cross sections $\sigma_{Pr}(\lambda)$ for native oat phyA,[47] and $\Phi_{Pr\rightarrow I700} = \Phi_{Pr\rightarrow Pfr} = 0.154$[6,48] were used.

The values for N_{phot} and the onset of the leveling-off calculated for both excitation wavelengths by the model function that assumes that a light-induced back reaction is not significant (Scheme 1) are much too high in comparison to the experimental data (Figure 2). Although the approximation with $\lambda_{exc} = 650$ nm is inacceptable only at higher photon densities, the model function throughout reflects in no way the experimental results with $\lambda_{exc} = 700$ nm. This disagreement argues against Scheme 1 as do also the $\Phi_{Pr\rightarrow I700}$ values calculated from ΔV^{satd} and b for this scheme (see Table 2). For $\lambda_{exc} = 650$ nm, the estimated $\Phi_{Pr\rightarrow I700}$ values are twice the experimental $\Phi_{Pr\rightarrow Pfr}$ value reported by Lagarias et al.[48] and, therefore, also in disagreement with Scurlock et al.[49] Furthermore, an unrealistic value of $\Phi_{Pr\rightarrow I700} > 1$ is obtained for $\lambda_{exc} = 700$ nm.

When Scheme 2 was applied instead, the agreement between the values derived from ΔV^{satd} and b at the two excitation wavelengths was excellent (see Table 2 for the calculated $\Phi_{I700\rightarrow Pr}$ values).

It should be pointed out that the uncertainty in $\Phi_{I700\rightarrow Pr}$ is relatively large. Taking into account relative errors of 10−20% for ΔV^{satd}, 5% for b, 7.5% for σ_{Pr},[47] 3% for $\Phi_{Pr\rightarrow Pfr}$,[48] 12% for σ_{I700} at 650 nm, 6% for σ_{I700} at 700 nm,[16] and 20% for ΔV_e,[6] overall relative errors of 40−60% result for $\Phi_{I700\rightarrow Pr}$, depending on the equations used. Despite these large error limits, there is good agreement with all data based on Scheme 2. Therefore, an average value for $\Phi_{I700\rightarrow Pr} = 0.22 \pm 0.12$ is obtained if it is assumed that the quantum yields are independent of excitation wavelength and that $\Phi_{Pr\rightarrow I700}$ equals $\Phi_{Pr\rightarrow Pfr}$. For a value of $\Phi_{Pr\rightarrow I700}$ larger than 0.154,[6] $\Phi_{I700\rightarrow Pr}$ would decrease according to eq 8.

TABLE 3: ΔV^{satd} and b Values for PYP, Derived from Figure 3 and Eq 2, Together with Literature Values for the pG and pR Absorption Cross Sections (σ_{pG} and σ_{pR}, Respectively) and the Number of PYP Molecules N_{PYP} in the Excited Volume

λ_{exc} (nm)	σ_{pG} (cm^{-2})[a] $\times 10^{16}$	σ_{pR} (cm^{-2})[b] $\times 10^{17}$	b (cm^{-2}) $\times 10^{17}$	ΔV^{satd} (mL) $\times 10^{10}$	N_{PYP} $\times 10^{-13}$
446	1.74	7.31	5.56	2.99	1.10
460	1.32	7.49	5.38	8.30	2.80
480	0.22	6.85	1.21	1.16	0.78

[a] Values taken from Meyer et al.[50] [b] Values taken from Hoff et al.[30]

TABLE 4: Quantum Yields of PYP for the Forward Reaction, $\Phi_{pG\rightarrow pR}$ and the Back Reaction $\Phi_{pR\rightarrow pG}$ Derived from ΔV^{satd} and b Based in Schemes 1 and 2

Scheme 1 (without Photoequilibrium)

λ_{exc} (nm)	$\Phi_{pG\rightarrow pR}$[a]	$\Phi_{pG\rightarrow pR}$[b]
446	0.32	0.30
460	0.41	0.29
480	0.55	0.54

Scheme 2 (with Photoequilibrium)

λ_{exc} (nm)	$\Phi_{pR\rightarrow pG}$[a]	$\Phi_{pR\rightarrow pG}$[b]
446	0.03	0
460	0.06	*c*
480	0.08	0.06

[a] Calculated from b. [b] Calculated from ΔV^{satd}. [c] A meaningless value (−0.01) was obtained.

Photoactive Yellow Pigment. The data analysis is more simple for PYP than for phyA. As already discussed, the PYP saturation experiments can be analyzed with eq 2. Since only a single photoproduct, pR, has been observed on the nanosecond time scale and in femtosecond transient absorption studies (a pR-like intermediate develops within 3 ps[29]), B in Schemes 1 and 2 is to be considered as the pR intermediate of the PYP photocycle.

Fitting functions using eq 2 are shown in Figure 3 together with the experimental data points obtained upon excitation at 446 and 460 nm. The values of b and ΔV^{satd} are given in Table 3 together with the literature values for σ_{pG} and σ_{pR}.[30,50] Figure 3 also exhibits the simulated model functions based on Scheme 1 and using σ_{pG}, σ_{pR}, and $\Phi_{pG\rightarrow pR} = 0.35$.[8] For both wavelengths, the model function shows good agreement with the experimental data. Scheme 1 affords an average value of $\Phi_{pG\rightarrow pR} = 0.33 \pm 0.05$ (Table 4). The $\Phi_{pG\rightarrow pR}$ value obtained with excitation at 480 nm, however, differed considerably: $\Phi_{pG\rightarrow pR} = 0.55 \pm 0.1$ (Table 4).

The difference in these values indicates that Scheme 1 is not appropriate for describing the saturation behavior and that the photochemical back reaction pR → pG occurs. We therefore analyzed the three experiments on the basis of Scheme 2, choosing the minimal $\Phi_{pG\rightarrow pR}$ value consistent with the flash-photolysis data, i.e., $\Phi_{pG\rightarrow pR} \geq \Phi_{pG\rightarrow pB} = 0.30$ [8] and calculated $\Phi_{pR\rightarrow pG}$ values to be between 0 and 0.08 (Table 4). Since σ_{pR} at $\lambda_{exc} = 480$ nm is 3 times larger than σ_{pG}, the photoreaction pR → pG should be more pronounced at this excitation wavelength. Accordingly, the $\Phi_{pR\rightarrow pG}$ value is estimated to equal 0.07 ± 0.04 at $\lambda_{exc} = 480$ nm.

We therefore conclude that Scheme 2 describes the photoreaction of PYP properly but that the back reaction pR → pG

is much less efficient than the forward reaction pG → pR; i.e., the ratio $\Phi_{pR\rightarrow pG}/\Phi_{pG\rightarrow pR}$ is around 0.2.

The LIOAS saturation experiments in this study strongly suggest that $\Phi_{pG\rightarrow pR} = 0.30-0.35$, which is very close to the quantum yield for the formation of the second intermediate pB ($\Phi_{pG\rightarrow pB} = 0.35$ [8]). Thus, the step pR → pB proceeds with about unity efficiency. Our study confirms the discrepancy with the earlier value of $\Phi_{pG\rightarrow pB} = 0.64$, claimed to have been obtained from ground-state bleaching recovery as well,[32] which we already judged as erroneous on the basis of low-fluence transient absorption results.[8] A more recent study also reported a value of ca. 0.35 for $\Phi_{pG\rightarrow pR}$.[29]

The low value of 0.07 for $\Phi_{pR\rightarrow pG}$ is compatible with absorption studies, which show that at least two primary products can be trapped at low temperature. One of these exhibits a red-shifted absorption and has been postulated to be the equivalent to pR at room temperature. This transient could be phototransformed back to pG upon excitation at 500 nm.[33] The low quantum yield for the back photoreaction should suffice to revert a low-temperature pR to ground-state pG upon excitation at the appropriate wavelength. However, the red shift in absorption from the room-temperature pR to the low-temperature intermediate is 20−30 nm, whereas the pG spectrum upon lowering the temperature is shifted only by 2 nm.[33] The intermediate trapped at low temperature and the room-temperature pR might therefore just as well be different; e.g., the low-temperature transient might precede pR and remain undetected at the physiological temperature.

Conclusion

The fluence dependence of the optoacoustic signal at $T_{\beta=0}$, i.e., of the structural volume change, for photoreceptors with isomerizable chromophores (phyA and PYP in this study) yields accurate information about the photochromic equilibrium between the starting compound and the first intermediate(s).

For phyA, the quantum yield of the photochemical back reaction ($\Phi_{I700\rightarrow Pr} = 0.22 \pm 0.12$) is about 1.4 times larger than that for the forward reaction ($P_r \rightarrow I_{700}$). This explains the establishment of the photoequilibrium $P_r \rightarrow I_{700}$ already at very low fluences and even at excitation wavelengths where the P_r absorption is higher than that of I_{700}.

For PYP, the photochemical back reaction (pR → pG) is of minor importance, with a quantum yield 5 times smaller than that of the forward reaction (pG → pR). The present LIOAS experiments allow us to estimate a value of 0.30−0.35 for the primary quantum yield $\Phi_{pG\rightarrow pR}$, in agreement with our previous value for $\Phi_{pG\rightarrow pB}$,[8] which indicates that the second step in the PYP photocycle, pR → pB, has about unity efficiency.

From the ratios of the quantum yields for the forward and reverse photoreactions ($\Phi_{A\rightarrow B}/\Phi_{B\rightarrow A}$) = 0.7 for phyA and 5 for PYP, we conclude that the protein-chromophore interactive changes are quite different in the two chromoproteins. In phyA the protein conformation is probably not extensively changed, since the trans → cis back isomerization is relatively favorable.

In contrast, an irreversible protein conformational change seems to take place on the picosecond time scale in PYP, which hinders the photoreversion of the chromophore and directs the protein forward into the photocycle.

The results of this work regarding the photoequilibrium do not have any direct physiological implication, since the photon densities used in the laboratory are far higher than those in nature. However, the results offer, in addition to quantitative parameters of the phototransformation, topology-related information about the first intermediates concerning the protein surrounding the chromophore.

Acknowledgment. We thank Peter Schmidt for helpful discussions, Willi Schlamann for the phyA preparations, and Robert Cordfunke for the PYP preparations. The oat seedlings were grown in facilities offered by L. Lindgens GmbH., Mülheim an der Ruhr.

References and Notes

(1) Kochendoerfer, G.; Mathies, R. A. *Isr. J. Chem.* **1995**, *35*, 211−226.

(2) Spudich, J. L.; Zacks, D. N.; Bogomolni, R. A. *Isr. J. Chem.* **1995**, *35*, 495−513.

(3) Kort, R.; Vonk, H.; Xu, X.; Hoff, W. D.; Crielaard, W.; Hellingwerf, K. J. *FEBS Lett.* **1996**, *382*, 73−78.

(4) Braslavsky, S. E.; Gärtner, W.; Schaffner, K. *Plant, Cell Environ.* **1997**, *20*, 700−706.

(5) Balashov, S. P. *Isr. J. Chem.* **1995**, *35*, 415−428.

(6) Gensch, T.; Churio, M. S.; Braslavsky, S. E.; Schaffner, K. *Photochem. Photobiol.* **1996**, *63*, 719−725.

(7) Gensch, T. Ph.D. Thesis, Heinrich-Heine-Universität, Düsseldorf, and MPI für Strahlenchemie, Mülheim/Ruhr, 1996.

(8) van Brederode, M.; Gensch, T.; Hoff, W. D.; Hellingwerf, K. J.; Braslavsky, S. E. *Biophys. J.* **1995**, *68*, 1101−1109.

(9) Callis, J. B.; Parson, W. W.; Gouterman, M. *Biochim. Biophys. Acta*. **1972**, *267*, 348−362.

(10) Braslavsky, S. E.; Heibel, G. E. *Chem. Rev.* ***1992***, *92*, 1381−1410.

(11) Malkin, S.; Churio, M. S.; Shochat, S.; Braslavsky, S. E. *J. Photochem. Photobiol., B* **1994**, *23*, 79−85.

(12) Puchenkov, O. V.; Kopf, Z.; Malkin, S. *Biochim. Biophys. Acta* **1995**, *1231*, 197−212.

(13) (a) Whitelam, G. C.; Haberd, N. P. *Plant, Cell Environ.* **1994**, *17*, 615−625. (b) Quail, P. H.; Boylan, M. T.; Parks, B. M.; Short, T. W.; Xu, Y.; Wagner, D. *Science* **1995**, *268*, 675−680.

(14) Rüdiger, W.; Thümmler, F. *Angew. Chem., Int. Ed. Engl.* **1991**, *30*, 1216−1228.

(15) Sineshchekov, V. A. *Biochim. Biophys. Acta*. **1995**, *1228*, 125−164.

(16) Zhang, C.-F.; Farrens, D. L.; Björling, S. C.; Song, P.-S.; Kliger, D. S. *J. Am. Chem. Soc.* **1992**, *114*, 4569−4580.

(17) Scurlock, R. D.; Evans, C. H.; Braslavsky, S. E.; Schaffner, K. *Photochem. Photobiol.* **1993**, *58*, 106−115.

(18) Kruk, A. B.; Krylov, K.; Lapko, V. N.; Dzhagarov, B. M.; Volotovskii, I. D. *Biofizika* **1996**, *41*, 299−305.

(19) Savikhin, S.; Wells, T.; Song, P.-S.; Struve, W. S. *Biochemistry* **1993**, *32*, 7512−7518.

(20) Kandori, H.; Yoshihara, K.; Tokutomi, S. *J. Am. Chem. Soc.* **1992**, *114*, 10958−10959.

(21) Holzwarth, A. R.; Venuti, E.; Braslavsky, S. E.; Schaffner, K. *Biochim. Biophys. Acta* **1992**, *1140*, 59−68.

(22) Hermann, G.; Lippitsch, M. E.; Brunner, H.; Aussenegg, F. R.; Müller, E. *Photochem. Photobiol.* **1990**, *52*, 13−18.

(23) (a) Pratt, L. H.; Inoue, Y.; Furuya, M. *Photochem. Photobiol.* **1984**, 39, 241−246. (b) Scheuerlein, R.; Braslavsky, S. E. *Photochem. Photobiol.* **1985**, *42*, 173−178. (c) Inoue, Y.; Furuya, M. *Plant Cell Physiol.* **1985**, *26*, 813−819.

(24) Sprenger, W. W.; Hoff, W. D.; Armitage, J. P.; Hellingwerf, K. J. *J. Bacteriol* **1993**, *175*, 3096−3104.

(25) Hoff, W. D.; Düx, P.; Hård, K.; Devreese, B.; Nugteren-Roodzant, I. M.; Crielaard, W.; Boelens, R.; Kaptein, R.; van Beeumen, J.; Hellingwerf, K. J. *Biochemistry* **1994**, *33*, 13959−13962.

(26) Baca, M.; Borgstahl, G. E. O.; Boissinot, M.; Burke, P. M.; Williams, D. W. R.; Slater, K. A.; Getzoff, E. D. *Biochemistry* **1994**, *33*, 14369−14377.

(27) Kim, M.; Mathies, R. A.; Hoff, W. D.; Hellingwerf, K. J. *Biochemistry* **1995**, *34*, 12669−12672.

(28) Meyer, T. E.; Tollin, G.; Causgrove, T. P.; Cheng, P.; Blankenship, R. E. *Biophys. J.* **1991**, *59*, 988−991.

(29) Baltuska, A.; van Stokkum, I. H. M.; Kroon, A.; Monshouwer, R.; Hellingwerf, K. J.; Van Grondelle, R. *Chem. Phys. Lett.* **1997**, *270*, 263−266.

(30) Hoff, W. D.; van Stokkum, I. H. M.; van Ramesdonk, H. J.; van Brederode, M.; Brouwer, A. M.; Fitch, J. C.; Meyer, T. E.; van Grondelle, R.; Hellingwerf, K. J. *Biophys. J.* **1994**, *67*, 1691−1705.

(31) Hoff, W. D.; Matthijs, H. C. P.; Schubert, H.; Crielaard, W.; Hellingwerf, K. J. *Biophys. Chem.* **1995**, *56*, 193−199.

(32) Meyer, T. E.; Tollin, G.; Hazzard, J. H.; Cusanovich, M. A. *Biophys. J.* **1989**, *56*, 559−564.

(33) (a) Hoff, W. D.; Kwa, S. L. S.; van Grondelle, R.; Hellingwerf, K. J. *Photochem. Photobiol.* **1992**, *56*, 529−539. (b) Imamoto, Y.; Kataoka, M.; Tokunaga, F. *Biochemistry* **1996**, *35*, 14047−14053.

(34) Brock, H.; Ruzsicska, B. P.; Arai, T.; Schlamann, W.; Holzwarth, A. R.; Braslavsky, S. E.; Schaffner, K. *Biochemistry* **1987**, *26*, 1412−1417.

(35) Indig, G. L.; Jay, D. G.; Grabowski, J. J. *Biophys. J.* **1992**, *61*, 631−638.

(36) Kell, G. S. *J. Chem. Eng. Data* **1967**, *12*, 66−69.

(37) (a) Nitsch, C.; Schatz, G.; Braslavsky, S. E. *Biochim. Biophys. Acta* **1989**, *975*, 88−95. (b) Strassburger, J.; Gärtner, W.; Braslavsky, S. E. *Biophys. J.* **1997**, *72*, 2294−2303.

(38) Debye, P. *Polar Molecules*; Dover Publications: New York, Dover 1929; pp 77−85.

(39) Srivastava, A.; Doraiswamy, S. *J. Chem. Phys.* **1995**, *103*, 6197−6205 and references therein.

(40) Kawato, S.; Kinosita, K. *Biophys. J.* **1981**, *36*, 277−296.

(41) Nagle, J. F.; Bhattacharjee, S. M.; Parodi, L. A.; Lozier, R. H. *Photochem. Photobiol.* **1983**, *38*, 331−339.

(42) Kliger, D. S.; Horwitz, J. S.; Lewis, J. W.; Einterz, C. M. *Vision Res.* **1984**, *24*, 1465−1470.

(43) Jones, A.; Erickson, H. P. *Photochem. Photobiol.* **1989**, *49*, 479−483.

(44) Nakasako, M.; Wada, M.; Tokutomi, S.; Yamamoto, K. T.; Sakai, J.; Kataoka, M.; Tokunaga, F.; Furuya, M. *Photochem. Photobiol.* **1990**, *52*, 3−12.

(45) Transient absorption experiments with linearly and circularly polarized excitation beams in fact indicate a rotation time slower than 50 ns for the phyA dimer (unpublished results by Schmidt, P., 1996).

(46) Note that the product bN_{phot} is a measure for the saturation. Thus, $bN_{phot} = 1$ indicates that 63% [with neither photoselection nor photochemical back reaction, at uniform photon distribution, eq 2] or 50% [with photoselection but without back reaction, at uniform photon distribution, eq 11] of all molecules in the illuminated volume have undergone phototransformation.

(47) Kelly, J. M.; Lagarias, J. C. *Biochemistry* **1985**, *24*, 6003−6010.

(48) Lagarias, J. C.; Kelly, J. M.; Cyr, K. L.; Smith, W. O., Jr. *Photochem. Photobiol.* **1987**, *46*, 5−13.

(49) Scurlock, R. D.; Braslavsky, S. E.; Schaffner, K. *Photochem. Photobiol.* **1992**, *57*, 690−696.

(50) Meyer, T. E.; Yakali, E.; Cusanovich, M. A.; Tollin, G. *Biochemistry* **1987**, *26*, 418−423.